Fluorescence Relaxation of Proflavin–Deoxyribonucleic Acid Interaction. Kinetic Properties of a Base-Specific Reaction†

Jean Ramstein,‡ Måns Ehrenberg,* and Rudolf Rigler

ABSTRACT: The kinetics of proflavin binding to *Micrococcus lysodeicticus* deoxyribonucleic acid (DNA) [(G-C) content 72%], to *Bacillus megaterium* DNA [(A-T) content 70%], and to the polydeoxyribonucleotides poly[d(G-C)] and poly[d(A-T)] was studied with fluorescence temperature-jump methods. Poly[d(A-T)] binds proflavin in a two-step reaction with a preequilibrium. Poly[d(G-C)] is characterized by a bimolecular reaction. The binding of acridines to natural DNAs is shown to be characterized by different types of sites whose properties depend on the base composition. The sites have considerable enthalpic differences which result in exchange of dye molecules between them when the temperature is changed. Also, on natural DNAs A-T base pairs are associated with a rapidly equilibrating external complex which is absent or much weaker for G-C base pairs.

Acridines are dye molecules with a wide spectrum of biological properties. Apart from their use as antibacterial and antimalarial agents (Albert, 1968), they are interesting because of their mutagenic properties (Crick et al., 1961; Brenner et al., 1961). Some acridines such as quinacrine and proflavin have been used to visualize defined regions in eukaryotic chromosomes (Caspersson et al., 1969). The interaction between deoxyribonucleic acid (DNA) and various acridines has therefore been extensively studied.

Proflavin has two binding modes on DNA with different affinity. Most experiments have been focused on the strong binding mode which has been related to the biological activity of the dye. It has been proposed that this binding mode structurally corresponds to an intercalation of proflavin between two adjacent base pairs where the plane of the dye is parallel to the plane of the base pairs (Lerman, 1961). The base pairs have to be separated by 3.4 Å to accommodate an intercalated dye molecule. Evidence in favor of such a mechanism has been reviewed by Blake & Peacocke (1968) and by Gale et al. (1972). Support for intercalation has recently come from X-ray data of complexes formed between self-complementary dinucleoside phosphates and acridine dyes or ethidium bromide (Seeman et al., 1974; Tsai et al., 1977; Jain et al., 1977; Sobell et al., 1977; Berman et al., 1977). However, in the case of native DNA the detailed geometry of the intercalation complex is still unknown.

In previous studies (Ramstein et al., 1972, 1973) the effect of proflavin on the hydrodynamic properties of DNA was investigated with linear dichroism and viscosity measurements. It was shown that a high (A-T) content of the DNA molecules leads to a high extent of contour lengthening when proflavin is bound. This strongly indicated that the base composition of DNA influences the geometry of the binding mode.

Li & Crothers (1969), using temperature jump with absorption detection, showed that proflavin binds to calf-thymus DNA in two steps. A rapidly formed precomplex is followed by an intercalated state of the dye. Measurements with the same technique on DNA with a higher (G-C) content (Ramstein & Leng, 1975), however, indicated that proflavin binds to DNA in a single step. It was therefore assumed that, in addition to the intercalation complex C_{int}, there exists a complex C_I of unknown structure whose affinity for proflavin is higher in (G-C)-rich than in (A-T)-rich DNA and which does not influence the contour length. This would account for an apparent single-step binding in (G-C)-rich DNA as well as for a more pronounced effect of proflavin on the contour length of (A-T)-rich DNA. The interpretation of previous investigations (Ramstein & Leng, 1975) may be summarized as shown in Scheme I. Implicit in Scheme I is a mechanism which enhances the affinity of proflavin to C_I as the (G-C) content increases. This is not a satisfactory situation, and in the present investigation we have used temperature jump with fluorescence detection in order to clarify further the role of base composition in the interaction between DNA and proflavin. Two synthetic DNAs, poly[d(G-C)] and poly[d(A-T)], were investigated, as well as DNA from *Micrococcus lysodeicticus* [*M.l.*, 72% (G-C)] and from *Bacillus megaterium* [*B.m.*, 30% (G-C)].

Scheme I

$$\text{Pro} + \text{DNA} \rightleftharpoons C_I \rightleftharpoons C_{int}$$

The quantum yield of proflavin is low in (G-C)-rich regions while it is high in (A-T)-rich regions of DNA (Weill, 1965; Thomes et al., 1969; Pachmann & Rigler, 1972). Therefore, fluorescence detection is ideally suited for an investigation of base selectivity in the binding of proflavin to DNA. Furthermore, the high sensitivity of the technique allows a high phosphate to dye ratio also at low DNA concentrations. Effects related to interactions between dye molecules are therefore minimized.

Our findings, which in particular contain a long relaxation time previously not observed (Li & Crothers, 1969) or one which has been detected with a very small amplitude (Ramstein & Leng, 1975), have led to a reinterpretation of the binding mechanism and therefore to a revision of Scheme I: There exist different regions in DNA with different kinetics of proflavin binding. One is similar to what is found for poly[d(A-T)], and the other is similar to the binding mechanism of poly[d(G-C)]. The exchange of dye molecules between (A-T)- and (G-C)-rich regions is characterized by a long

† From the Department of Medical Biophysics, Karolinska Institutet, S-104 01 Stockholm, 60, Sweden. *Received July 19, 1979.* This paper is dedicated to Torbjörn Caspersson on the occasion of his 70th birthday. This work was supported by grants from the Swedish Cancer Society and from the Swedish Natural Science Research Council. J.R. benefitted from the French–Swedish Scientific Exchange Program organized by the Swedish Natural Science Research Council and Centre de Recherche Scientifique.

‡ Permanent address: Centre de Biophysique Moléculaire, Orléans, France.

0006-2960/80/0419-3938$01.00/0

relaxation time which is unaffected by the DNA phosphate concentration.

Materials and Methods

Materials

Proflavin was purchased from British Drug Houses and used without further purification.

DNAs. The synthetic polydeoxyribonucleotides poly[d(G-C)] and poly[d(A-T)] were purchased from Boehringer, Mannheim. Double-helix formation was checked by observing the melting transition. The hyperchromicities of poly[d(G-C)] and of poly[d(A-T)] were 31% at $\lambda = 275$ nm and 50% at $\lambda = 260$ nm, respectively, in agreement with Wells et al. (1970). For concentration determinations the extinction coefficients 6800 M^{-1} cm^{-1} for poly[d(A-T)] at 260 nm and 8400 M^{-1} cm^{-1} for poly[d(G-C)] at 254 nm were used (Wells et al., 1970). *M.l.* DNA [72% (G-C)] and *B.m.* DNA [30% (A-T)] were purified according to Ramstein et al. (1971).

All DNA–proflavin complexes were prepared in a standard buffer consisting of 0.1 M sodium chloride, 10^{-2} M Tris, pH 7.0, and 10^{-4} M EDTA. The phosphate to dye ratio [P]/[D] was kept equal to 100 or greater in order to exclude nearest-neighbor interactions of bound proflavin. For each phosphate concentration of native DNA an individual sample was prepared. For poly[d(G-C)] and poly[d(A-T)] the content of the temperature-jump cell was diluted and reused when the phosphate concentration of the sample was higher than 10^{-4} M. Otherwise, samples were prepared as for native DNA.

Methods

The fluorescence temperature-jump apparatus has been described in detail elsewhere (Rigler et al., 1974). The light source was a 200-W Hg lamp and the excitation wavelength 436 nm. The emission was passed through 495-nm cutoff filters (GG 495, G. Schott). The excitation path length of the temperature-jump cell was 7 mm. Temperature jumps of about 7 °C were obtained from a 30-kV capacitor discharge giving a heating time of ~ 18 μs. In all experiments reported here the final temperature was 17 °C after a temperature jump. With the large [P]/[D] ratios used all rate equations can be linearized even for large perturbations of the chemical equilibrium. The fluorescence signal was, after amplification, digitized and stored in a transient recorder memory (Biomation 802). The raw data were transferred to tape and subsequently evaluated with respect to relaxation times and amplitudes by using nonlinear regression analysis (Marquardt, 1963; Meeter, 1964). The initial values of the parameters were obtained from an analogue exponential simulator (Rigler et al., 1974).

Results

All fluorescence relaxation curves showed a rapid intensity decrease after a temperature jump. This change, faster than the time resolution of the instrument, was probably caused by a temperature-dependent variation of the quantum yield of proflavin and will not be discussed further.

M.l. DNA–Proflavin and B.m. DNA–Proflavin Complexes. The relaxation signal of the *M.l.* DNA–proflavin system displays two distinct parts: a fast increase of the fluorescence intensity with the relaxation time τ_{fast} is followed by a slow decrease characterized by the relaxation time τ_{slow}. The variation of the two relaxation times with phosphate concentration is shown in Figures 1A and 2A. $1/\tau_{fast}$ depends linearly on the phosphate concentration, whereas $1/\tau_{slow}$ is approximately constant. The relative amplitude corresponding to τ_{fast} has a maximum at 0.5×10^{-4} M (Figure 1B). The relative amplitude corresponding to τ_{slow} decreases to a constant value with increasing phosphate concentration (Figure 2B).

Also, for the *B.m.* DNA–proflavin complex the relaxation signal has two distinct parts characterized by a fast (τ_{fast}) and a slow (τ_{slow}) relaxation time. Here, in contrast to the *M.l.* case, the fluorescence intensity increases in both relaxation processes. $1/\tau_{fast}$ varies almost linearly at low phosphate concentration and reaches a plateau at high phosphate concentration (Figure 1A). $1/\tau_{slow}$ is approximately constant (Figure 2A). The corresponding relative amplitudes are shown in Figures 1B and 2B. The relative amplitude of τ_{fast} has a maximum at a phosphate concentration of 0.4×10^{-4} M, whereas the relative amplitude of τ_{slow} is constant.

In previous studies on *M.l.* DNA with absorption detection (Ramstein & Leng, 1975) a relaxation time corresponding to τ_{fast} was found. A slow relaxation process was present, yet its amplitude was too small to allow a detailed interpretation. Proflavin binding to calf-thymus DNA is characterized by a relaxation time very similar to τ_{fast} of *B.m.* DNA as shown by Li & Crothers (1969). They found no long relaxation time but detected a rapid process where the inverse relaxation time varies linearly with phosphate concentration. This fast binding step could not be seen with fluorescence detection either for *B.m.* or for *M.l.* DNA. The influence of base composition on the proflavin kinetics encountered so far made it of considerable interest to investigate the two pure cases poly[d(G-C)] and poly[d(A-T)].

Poly[d(G-C)]–Proflavin and Poly[d(A-T)]–Proflavin Complexes. The fluorescence signal of the binding of proflavin to poly[d(G-C)] has one relaxation time whose inverse varies linearly with the phosphate concentration (Figure 3A). A bimolecular reaction scheme summarizes the experiments (see Scheme II) where the relaxation time is given by

Scheme II

$$\text{poly[d(G-C)]} + \text{Pro} \underset{k_{-2}}{\overset{k_2}{\rightleftharpoons}} C_I$$

$$1/\tau = k_2([\text{P}] + [\text{Pro}]) + k_{-2} \qquad (1)$$

[P] and [Pro] are the concentrations of free phosphate and free proflavin, respectively. Experimentally determined values of k_2 and k_{-2} are listed in Table I. The relative amplitude of the signal is positive and has a maximum at a phosphate concentration of 1.0×10^{-4} M.

Also, in the poly[d(A-T)]–proflavin system the chemical relaxation process has one relaxation time. It tends toward a constant value when the phosphate concentration is large (Figure 3A). The binding is therefore not compatible with a single step as in the poly[d(G-C)] case but with a two-step mechanism where one step cannot be observed. The corresponding relative amplitude has a maximum at a phosphate concentration of 10^{-5} M (Figure 4B), which is small in relation to the poly[d(G-C)] case. This shift is primarily caused by the higher quantum yield of proflavin when it is bound to poly[d(A-T)] (cf. Appendix). The experiments on poly[d(A-T)] can be summarized in Scheme III where the first step equilibrates rapidly in relation to the second.

Scheme III

$$\text{poly[d(A-T)]} + \text{Pro} \overset{K_e}{\rightleftharpoons} C_e \underset{k_{-1}}{\overset{k_1}{\rightleftharpoons}} C_{int}$$

The relaxation time is given by

$$1/\tau = k_{-1} + k_1 K_e[\text{P}_0]/(1 + K_e[\text{P}_0]) \qquad (2)$$

with $[\text{P}_0]$ the input concentration of DNA phosphates when $[\text{P}] \gg [\text{Pro}]$. Using eq 2 we have estimated k_1, k_{-1}, and K_e

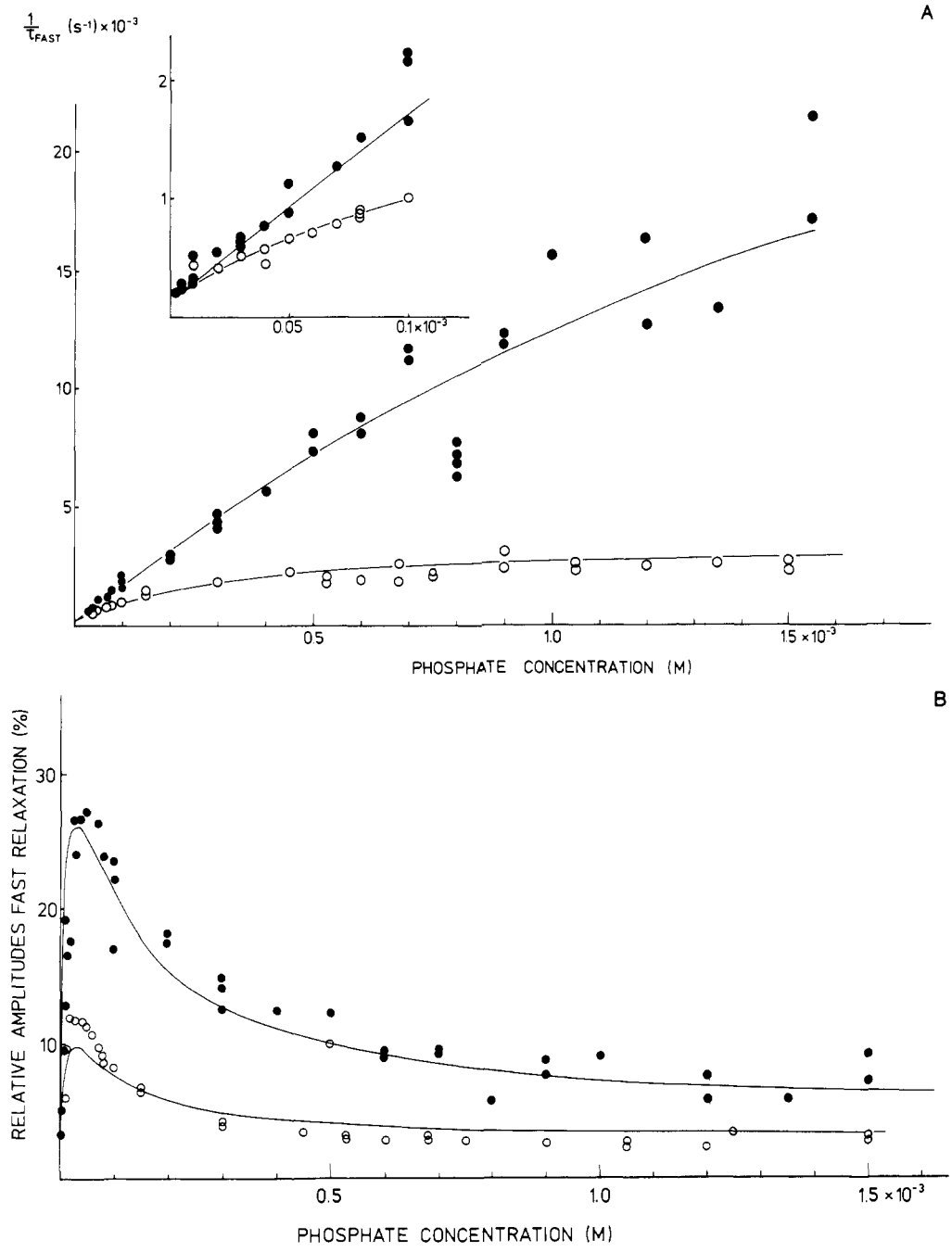

FIGURE 1: (A) Inverse of the short relaxation time as a function of phosphate concentration: *M.l.* DNA (●); *B.m.* DNA (○). (B) Relative amplitudes of the short relaxation time as a function of phosphate concentration: *M.l.* DNA (●); *B.m.* DNA (○).

from the experimentally determined relaxation times (Table I).

As far as the fast relaxation times are concerned, poly[d-(G-C)] resembles *M.l.* DNA, and poly[d(A-T)] behaves like *B.m.* DNA. No slow relaxation process is present either in the pure (A-T) or in the pure (G-C) case.

However, when the kinetics of a mixture of poly[d(A-T)] and poly[d(G-C)] is studied, a long relaxation time will emerge reflecting an exchange of dye molecules between the two polynucleotide types. We investigated the interaction between proflavin and a mixture of 70% poly[d(G-C)] and 30% poly-[d(A-T)] with an overall base composition coinciding with that of *M.l.* DNA. There is a short relaxation time whose inverse has an approximately linear DNA phosphate concentration dependence (Figure 3A). The long time is constant (Figure 4A). The amplitudes corresponding to the short and long relaxation times are shown in Figures 3B and 4B, respectively.

Scheme IV

$$\text{(G-C)} + \text{Pro} \underset{k_{-2}}{\overset{k_2}{\rightleftharpoons}} \text{C}_1$$

$$\text{(A-T)} + \text{Pro} \overset{K_e}{\rightleftharpoons} \text{C}_e \underset{k_{-1}}{\overset{k_1}{\rightleftharpoons}} \text{C}_{int}$$

The experiments on the mixture are summarized in Scheme IV. As shown in the Appendix, the short relaxation time is, at high phosphate concentration, given by

$$\frac{1}{\tau_{fast}} = \frac{k_1\alpha[P]K_e}{1 + \alpha[P]K_e} + \frac{k_2(1-\alpha)[P]}{1 + \alpha[P]K_e} + k_{-1}\left(\frac{k_1K_e\alpha}{k_1K_e\alpha + k_2(1-\alpha)}\right) + k_{-2}\left(\frac{k_2(1-\alpha)}{k_1K_e\alpha + k_2(1-\alpha)}\right) \quad (3)$$

and the long by

Table I[a]

	$k_2 \times 10^{-7}$ (M^{-1} s^{-1})	$k_{-2} \times 10^{-3}$ (s^{-1})	$k_1 \times 10^{-3}$ (s^{-1})	$k_{-1} \times 10^{-3}$ (s^{-1})	$K_e \times 10^{-3}$ (M^{-1})	K_1	$K_2 \times 10^{-5}$ (M^{-1})	ΔH (kcal)	$f \times 10^{-4}$ (M^{-1} cm^{-1})	α
poly[d(G-C)]	1.56 ± 0.04	0.17 ± 0.01					0.91 ± 0.07	$\Delta H_2 = -11$	$f_2 = 0.033 \pm 0.003$	
poly[d(A-T)]			3.6 ± 0.9	0.08 ± 0.01	4.6 ± 1.5	46 ± 20		$\Delta(H_1 + H_e) = -4$	$f_1 = 1.15 \pm 0.26$	
DNA	1.68 ± 0.06	0.12 ± 0.01	3.3 ± 0.6	0.20 ± 0.01	3.3 ± 0.5	16 ± 4	1.35 ± 0.15	$\Delta(H_1 + H_e) = -13$	$f_1 = 1.58$	$\alpha_{M.l.} = 0.09$
										$\alpha_{M.l.}{}^b = 0.03$
								$\Delta H_2 = -12.5$	$f_2 = 0.0327$	$\alpha_{B.m.} = 0.99$
										$\alpha_{B.m.}{}^b = 0.8$
M.l. DNA	1.42 ± 0.04	0.18 ± 0.01					0.78 ± 0.08	$\Delta H_2 = -10$		
B.m. DNA			2.9 ± 0.2	0.23 ± 0.04	3.5 ± 0.6	12 ± 3		$\Delta(H_1 + H_e) = -15$		

[a] Parameters of the row DNA were evaluated according to the scheme $x + y_2 \rightleftharpoons z_2$, $x + y_1 \rightleftharpoons e \rightleftharpoons z_1$ by fitting the eigenvalues in (A5) to the inverse relaxation times and by fitting (A25) and (A26) divided by (A17) to the relative amplitudes. Parameters of the rows *M.l.* DNA and *B.m.* DNA were obtained by analyzing the short relaxation times with the simplified mechanism $x + y_2 \rightleftharpoons (k_2\ k_{-2})\ z_2$ for *M.l.* DNA and $x + y_1 \rightleftharpoons (K_e)\ e \rightleftharpoons (k_1\ k_{-1})\ z_1$ for *B.m.* DNA. The fluorescence factors f_1 and f_2 are defined as $f_i = \epsilon_i Q_i$ ($i = 1$ or 2), where ϵ_i is the extinction coefficient and Q_i the quantum yield. f_1 and f_2 for poly[d(A-T)] and poly[d(G-C)], respectively, were estimated from amplitude analysis. f_1 and f_2 in the DNA column were obtained by assuming $\epsilon = 21\,000$ cm^{-1} M^{-1}, $Q = 0.78$, and $Q = 0.016$, respectively. [b] Values obtained from the amplitude analysis.

$$\frac{1}{\tau_{slow}} = k_{-1}\left(\frac{(1-\alpha)k_2}{k_1K_e\alpha + k_2(1-\alpha)}\right) + k_{-2}\left(\frac{\alpha k_1 K_e}{k_1K_e\alpha + k_2(1-\alpha)}\right) \quad (4)$$

where α is the (A-T) content. The relaxation times of the mixture have a close resemblance with those of *M.l.* DNA. This is suggestive and indicates that a scheme of type IV also may account for the binding of proflavin to native DNA.

In order to decide whether the observed relaxation kinetic behavior is typical only for proflavin, we have extended our studies to include the interaction between *B.m.* and *M.l.* DNA and a related acridine, quinacrine, which is used for chromosome identification (Caspersson et al., 1969). Since the amplitudes of the relaxation signals are much smaller in this case, the treatment is confined to a qualitative analysis. The results are shown in Figure 5; for both DNAs there is a long relaxation time which stays constant over the investigated concentration range. For *M.l.* DNA there is a fast relaxation time whose inverse varies linearly with phosphate concentration, and *B.m.* DNA displays a relaxation time reaching a plateau at high phosphate concentration. Thus the data are similar to those obtained with proflavin, and these suggest that the reaction mechanism discussed for proflavin is relevant also for the quinacrine case and, by inference, also for other similar dyes.

Discussion

Synthetic DNAs. Considerable differences exist in the chemical relaxation spectra of poly[d(A-T)] and poly[d(G-C)] interacting with proflavin. These differences suggest two main interpretations of the binding mechanism for the two synthetic and, thus, also for the natural DNAs. The first interpretation implies that proflavin intercalates in poly[d(A-T)] but not in poly[d(G-C)] and the second that proflavin intercalates in both species. In this work we shall favor the first alternative by arguments based on how the hydrodynamic properties of DNA change when it binds proflavin [c.f. Ramstein et al. (1972) and below]. However, the second alternative will also be given serious consideration since it cannot be excluded by present knowledge.

When proflavin interacts with poly[d(A-T)], the relaxation time (Figure 3A) reveals a preequilibrium. In analogy with the work of Li & Crothers (1969) and Ramstein & Leng (1975), the data may be summarized by a sequential scheme (see Scheme III). It was not possible to resolve the first step with fluorescence detection so we can only estimate the equilibrium constant $K_e = k_e/k_{-e}$ (Table I). For calf-thymus DNA the kinetics of a preequilibrium was resolved with absorption detection, and in analogy with that result we may assume that $k_e \approx 2 \times 10^7$ M^{-1} s^{-1} and $k_{-e} \approx 4 \times 10^3$ s^{-1}.

The complex C_e has an affinity which is higher than expected from electrostatic interactions alone (Li & Crothers, 1969). It must therefore be stabilized also by other forces. Instead of the sequential mechanism (Scheme III) a branched scheme is conceivable (see Scheme V). For explanation of the dependence on ionic strength of the kinetics [cf. Li & Crothers (1969)], the on rates q_1 and k_e must be combinations of electrostatic binding constants, weaker than K_e, and intramolecular transition rates to the intercalation site C_{int} or to the external complex C_e. q_1 in Scheme V is related to k_1 in Scheme III by $q_1 = K_e k_1$ so that, from Table I, $q_1 = 1.7 \times 10^7$ M^{-1} s^{-1}. At high phosphate concentration when association dominates over dissociation in *both* branches of Scheme V, the longest relaxation time describes the transfer of dye

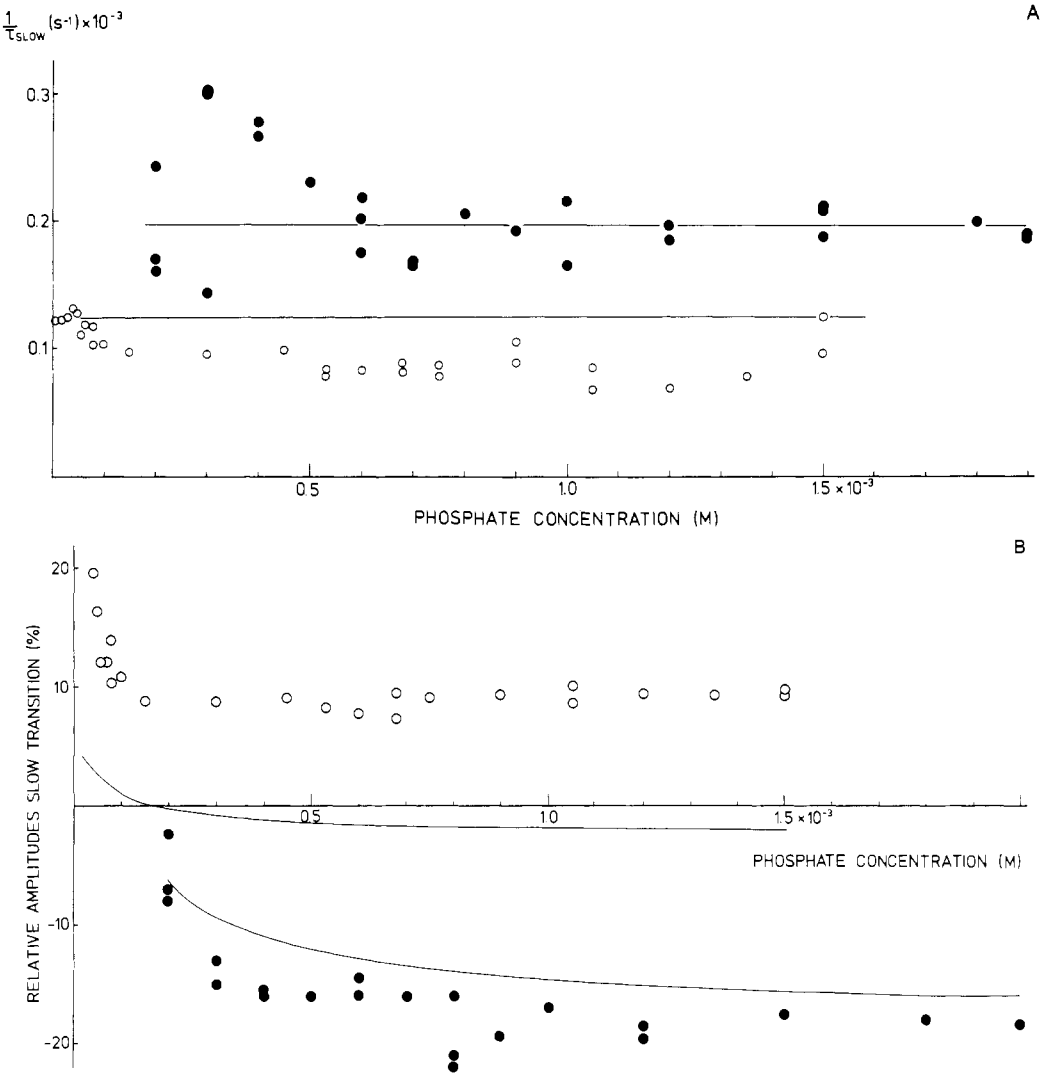

FIGURE 2: (A) Inverse of the long relaxation time as a function of phosphate concentration: *M.l.* DNA (●); *B.m.* DNA (○). (B) Relative amplitudes of the long relaxation time as a function of phosphate concentration: *M.l.* DNA (●); *B.m.* DNA (○).

Scheme V

$$\text{Pro} + \text{poly[d(A-T)]} \underset{q_{-1}}{\overset{q_1}{\rightleftharpoons}} C_{int}$$

$$\text{Pro} + \text{poly[d(A-T)]} \underset{k_{-e}}{\overset{k_e}{\rightleftharpoons}} C_e$$

molecules between C_e and C_{int} (cf. Appendix). Since $k_{-e} \gg k_{-1}$, this gives approximately

$$\frac{1}{\tau_{fast}} = k_{-e}\frac{q_1}{q_1 + k_e}$$

What in Scheme III is estimated as k_1 would therefore, if $q_1 = k_e$, appear as $k_{-e}/2$ in Scheme V. This is indeed the case for calf-thymus DNA (Li & Crothers, 1969; Ramstein & Leng, 1975). In the case of poly[d(G-C)] the chemical relaxation spectrum indicates a single step according to Scheme II.

At 17 °C the affinity of C_I is a factor of 2 smaller than the overall affinity K_eK_1 for C_{int} (Table I). The difference arises primarily from the off rates. k_{-2} is larger than k_{-1} and the overall association rates K_ek_1 and k_2 are almost identical. The enthalpic part of k_2 is large in relation to the enthalpic part of K_1K_e (Table I). The binding of proflavin to poly[d(A-T)] is therefore favored in relation to poly[d(G-C)] at high temperatures.

Scheme II deviates considerably from the original (Li & Crothers, 1969) kinetic intercalation scheme. This might reflect a new structural complex typical for (G-C) base pairs on the outside of the DNA helix. In comparison with the outer complex C_e found for poly[d(A-T)] C_I is a factor of 200 more stable (Table I). There is no experimental indication of additional steps in the binding. Therefore, if C_I is an outside complex, intercalation between (G-C) base pairs is to a large extent prohibited.

On the other hand, C_I might a priori also be an intercalated state of the dye. The occurrence of intercalation between (G-C) base pairs has been shown by X-ray studies (Berman et al., 1977, 1979). In favor of this hypothesis are the common features of Schemes V and II. A large structural similarity between C_I and C_{int} would explain why the association rates k_2 and q_1 as well as the equilibrium constants K_2 and Q_1 are similar. Furthermore, the similarity in absorption spectra (Ramstein & Leng, 1975) indicates equivalent binding modes. However, to explain the large differences which we observe for the enthalpies, it must be assumed that the properties of the intercalated state itself strongly depend on the actual combination of neighboring base pairs. For this, theoretical support has been given (Ornstein & Rein, 1979).

If poly[d(A-T)] and poly[d(G-C)] are mixed, there will be a kinetic coupling between the two reactions. A fast relaxation process appears which is a weighted average over the rates of (G-C) and (A-T) binding (see Appendix). Furthermore, a

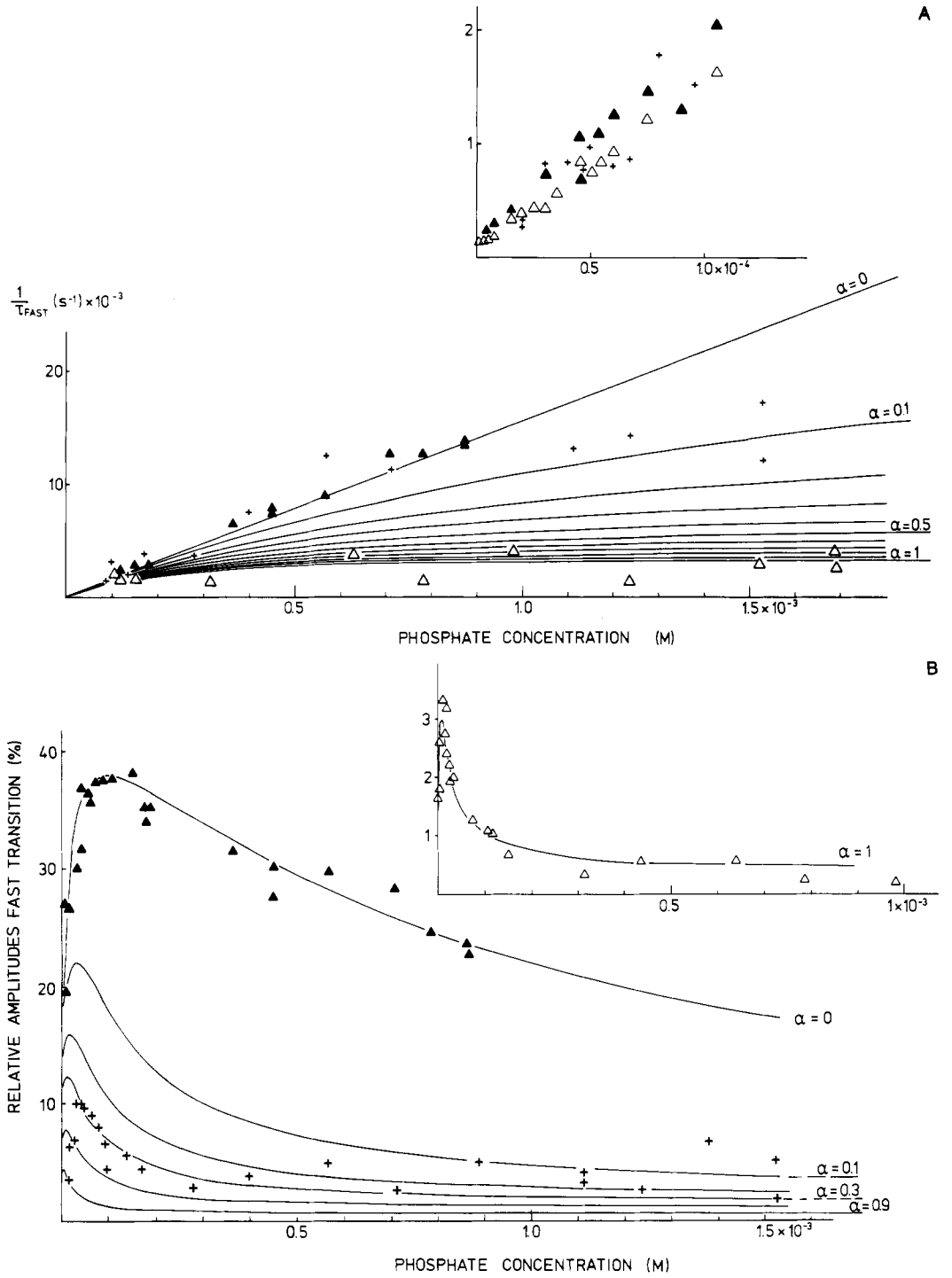

FIGURE 3: (A) Inverse of the short relaxation time as a function of phosphate concentration for different values of α [fraction of the number of poly[d(A-T)]-like binding sites]: poly[d(G-C)] (▲); poly[d(A-T)] (△); mixture of 70% poly[d(G-C)] + 30% poly[d(A-T)] (+). (B) Relative amplitudes of the short relaxation time as a function of phosphate concentration for different values of α: poly[d(G-C)] (▲); poly[d(A-T)] (△); mixture of 70% poly[d(G-C)] + 30% poly[d(A-T)] (+).

slow transition is present which arises from an exchange of dye molecules between (A-T) and (G-C) sites. The experiments on a mixture with 30% poly[d(A-T)] show that the long relaxation time is constant in accordance with theory up to at least 1.5 mM phosphate concentration. This behavior excludes a direct transfer between C_I and C_{int} as described for ethidium bromide by Bresloff & Crothers (1975).

We have used parameters determined from measurements on the pure poly[d(A-T)] and pure poly[d(G-C)] systems (Table I) together with eq A7, A29, and A30 to simulate experiments on mixtures with different (A-T) contents. The short relaxation times and their amplitudes as measured directly on the mixture and simulated are in good agreement (Figure 3). The simulation gives a qualitatively correct prediction of the behavior of the long relaxation times and their amplitudes (Figure 4). The observed deviations are due to a low precision in the determination of the off rate k_{-1} of poly[d(A-T)]. The fact that no slow relaxation process can be observed for either of the synthetic polynucleotides and that the slow relaxation process, which is present in the mixture, has important characteristics in common with the slow processes observed for the two natural DNAs strongly indicates that both *M.l.* and *B.m.* DNA have heterogeneous binding sites for proflavin.

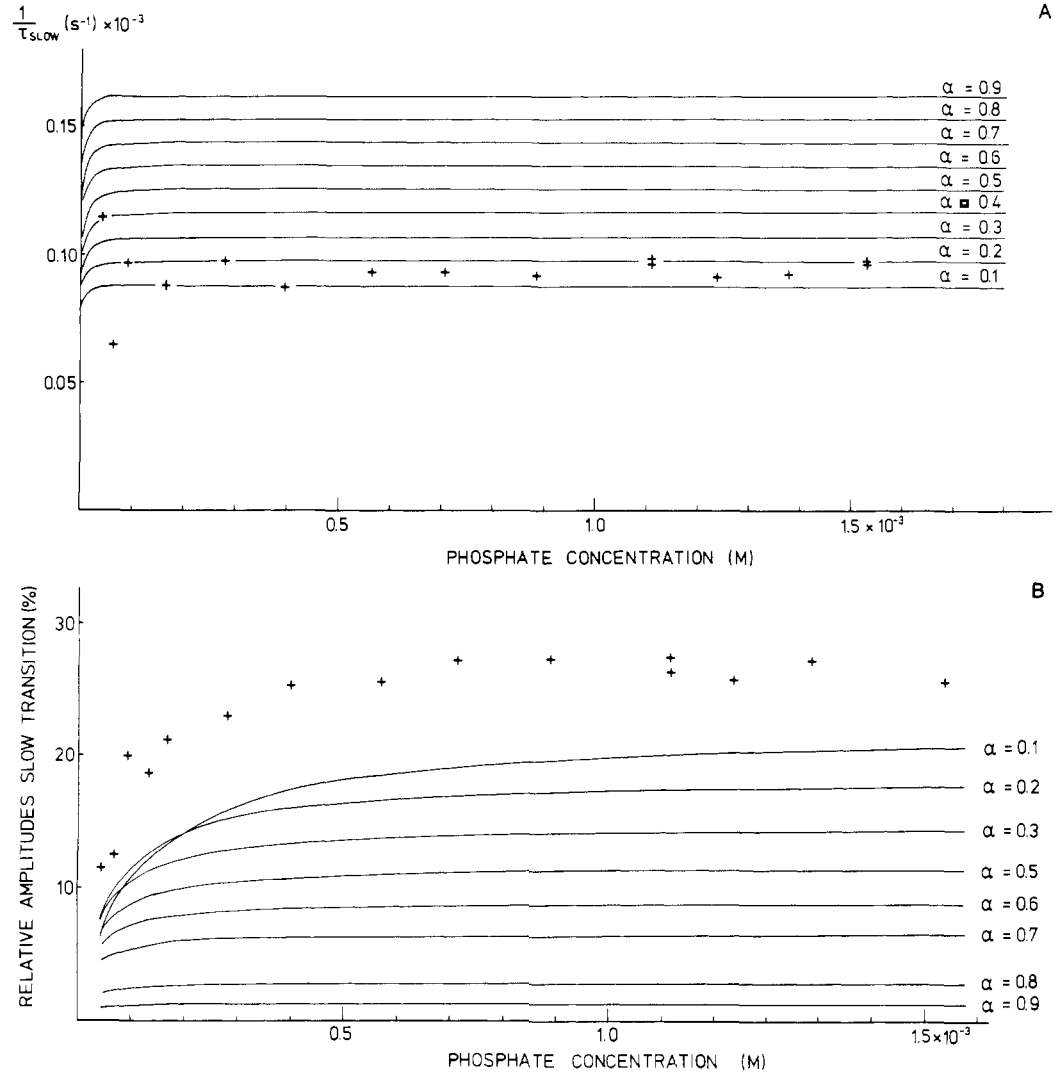

FIGURE 4: Inverse of the long relaxation time as a function of phosphate concentration for different values of α [fraction of the number of poly[d(A-T)]-like binding sites]: mixture of 70% poly[d(G-C)] + 30% poly[d(A-T)] (+). (B) Relative amplitudes of the long relaxation time as a function of phosphate concentration for different values of α: mixture of 70% poly[d(G-C)] + 30% poly[d(A-T)] (+).

Natural DNAs. The relaxation spectrum of the (A-T)-rich DNA from *B.m.* is with respect to the short relaxation time similar to the spectrum of poly[d(A-T)] (Figures 1 and 3). The long relaxation time (Figure 2A) has a positive amplitude (Figure 2B). When the temperature is increased, there is therefore a net transfer of dye molecules from a state of low to a state of high quantum yield. The (G-C)-rich DNA from *M.l.* has a fast relaxation time which is similar to $1/\tau_{fast}$ of poly[d(G-C)] (Figures 1 and 3). The long relaxation time (Figure 2A) has a negative amplitude (Figure 2B) which shows that a rise in temperature results in a net transfer of dye molecules from a state of higher to a state of lower quantum yield in contrast with the *B.m.* case. From these experiments it follows that also in natural DNAs primarily (A-T) base pairs are associated with an extra complex C_e. It is furthermore clear from the long relaxation times that there exist at least two thermodynamically different binding sites on natural DNA.

A detailed quantitative evaluation of the chemical relaxation spectra of *B.m* and *M.l.* DNA has been made with the simplifying assumption that there exist only two types of sites, one (A-T) like with a preequilibrium C_e and one (G-C) like with single chemical step (see Scheme IV). The result of this analysis is given in the column DNA of Table I. In Figures 1 and 2 the simulated chemical relaxation times and amplitudes are shown. The fit is satisfactory for the short relaxation times and their amplitudes (Figure 1) and acceptable for the long relaxation times (Figure 2A). However, the amplitudes of the long relaxation times cannot be fitted by such a simple model (Figure 2B). In order to accommodate the positive sign for *B.m.* and the negative sign for *M.l.* DNA, we found that a more complicated description is necessary.

In fact, if we make the natural assumption that a (G-C)-like site is always more quenched than an (A-T)-like site, we have to infer a higher enthalpy for (G-C) binding than for (A-T) binding in the case of *B.m.* DNA. This is in accordance with the exchange of dye molecules between poly[d(A-T)] and poly[d(G-C)] (Table I, Figure 4B). However, in the *M.l.* case the complex C_I must have a lower enthalpy than C_{int}.

We have thus established the existence of several different types of binding sites on natural DNAs. Their optical and thermodynamic properties have substantial differences as the large amplitudes which accompany the exchange of dye molecules show (Figure 2B).

Natural DNAs have several combinations of neighboring base pairs and underlying our measurements on *B.m.* and *M.l.* DNA are probably chemical relaxation spectra composed of the binding to and exchange between more than two different types of sites. Such a situation cannot be resolved by a direct approach as made here. A systematic study of the kinetics

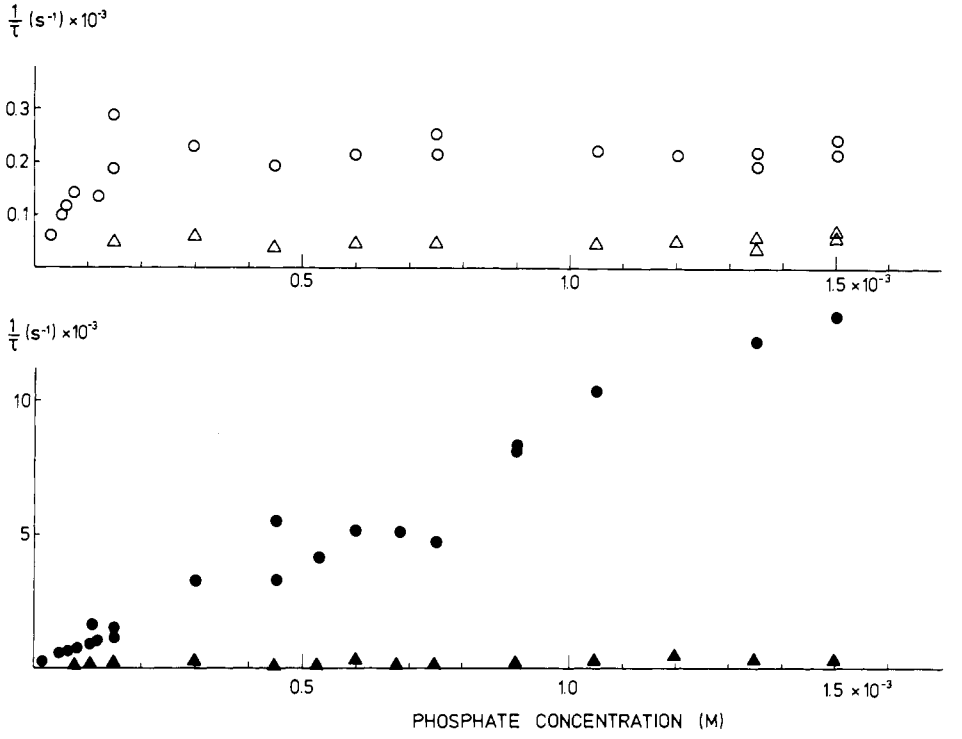

FIGURE 5: Inverse of the short and long relaxation times as a function of phosphate concentration for quinacrine–DNA systems: quinacrine–*B.m.* DNA, short relaxation time (○) and long relaxation time (△); quinacrine–*M.l.* DNA, short relaxation time (●) and long relaxation time (▲).

of synthetic polynucleotides with different sequences would be more suitable.

The exchange of proflavin molecules between different sites on DNA differs principally from a transfer mechanism proposed for ethidium bromide by Bresloff & Crothers (1975). In their case, two sites for ethidium with properties independent of base composition were postulated. The exchange of dye molecules between the sites was accelerated when the phosphate concentration increased. This indicated that there exists a direct pathway between the sites which can be activated by the interaction of two DNA molecules. Such an effect can be excluded for proflavin at phosphate concentrations below 1.5 mM. The long relaxation times for the natural DNAs (Figure 2A) as well as for the mixture of poly[d(A-T)] and poly[d(G-C)] (Figure 4A) show no tendency to decrease with increasing DNA concentration.

The long relaxation times $1/\tau_{slow}$ which have been detected here with large amplitudes (Figure 2) have not been seen (Li & Crothers, 1969) or have been detected with small amplitudes (Ramstein & Leng, 1975) in previous work. If proflavin binds near a (G-C) base pair, the fluorescence is markedly quenched. Binding to two (A-T) base pairs results in a small fluorescence enhancement in relation to the fluorescence of the free state. In contrast, the absorption spectra show no base composition dependence. This explains why the exchange flows are easily seen with fluorescence detection but not when absorption is used (cf. eq A32). We could not (cf. above) resolve the kinetics of the formation of the complex C_e neither for poly[d(A-T)] nor for *B.m.* DNA. If the rates and enthalpies are similar to what has been reported for calf-thymus DNA (Li & Crothers, 1969), a possible explanation is that when C_e is formed the decrease in absorption at 436 nm is compensated for by an equal increase in the quantum yield.

Viscosity measurements on DNAs with varying (A-T) content (Ramstein et al., 1972) show that proflavin induces a considerably larger elongation of the DNA chain for (A-T)-rich DNA as compared to (G-C)-rich DNA. This is a strong argument in favor of the hypothesis that the (G-C) complex C_1 is an external site and the (A-T) complex C_{int} is an intercalated structure proceeded by the stabilized electrostatic complex C_e according to Scheme IV.

However, it is conceivable that the effects of intercalation on the DNA contour length depend on the base pairs which constitute the intercalation site. The finding that different intercalating agents have different effects on the DNA structure suggests such a possibility (Hogan et al., 1979). If so, our data are also compatible with intercalation of proflavin between all combinations of base pairs.

Acknowledgments

We thank Professor C. Hélène for helpful discussions and Professor Grelet and Dr. Chatelin (Department of Microbiology, University of Orléans) for providing us with the *B. megaterium*. Róza Jakabffy provided expert help in data evaluation and Karin Dahlberg in preparing the manuscript.

Appendix

The relaxation kinetics of proflavin binding to DNA is characterized by two parallel coupled reactions

$$x + y_1 \underset{}{\overset{K_e}{\rightleftharpoons}} e \overset{k_1}{\rightleftharpoons} z_1$$

$$x + y_2 \overset{k_2}{\rightleftharpoons} z_2 \qquad \text{(A1)}$$

All expressions corresponding to the branched scheme

$$x + y_1 \overset{K_e}{\rightleftharpoons} e$$

$$x + y_1 \underset{q_{-1}}{\overset{q_1}{\rightleftharpoons}} z_1 \qquad \text{(A2)}$$

$$x + y_2 \underset{k_{-2}}{\overset{k_2}{\rightleftharpoons}} z_2$$

may directly be derived from those calculated for (A1) by the replacements $K_e k_1 = q_1$ and $K_e(k_1/k_{-1}) = Q_1$ as long as the relaxation of e can be regarded as rapid in relation to the other reactions. Proflavin, with the free concentration x, can interact

with an (A-T)-like site y_1, form a precomplex e, and enter an intercalated state z_1 or interact with a (G-C)-like site y_2 and form the complex z_2.

Denoting the total DNA phosphate concentration by c_0 and the fraction of (A-T) sites by α, then the total concentration of (A-T) sites is αc_0 and of (G-C) sites $(1 - \alpha)c_0$. All experiments in this work were performed in high phosphate excess over dye, i.e., $x_0 \ll c_0$, where x_0 is the total proflavin concentration. Therefore the free concentrations of (A-T) sites and (G-C) sites are approximately equal to their total concentrations:

$$y_1 = \alpha c_0 \qquad y_2 = (1 - \alpha)c_0 \tag{A3}$$

When preequilibrium is established in (A1), there remain two independent differential equations. To these correspond two eigenvalues which, with the definitions

$$k_1' = \frac{k_1 \alpha c_0 K_e}{1 + \alpha c_0 K_e}$$

$$k_2' = \frac{k_2(1 - \alpha)c_0}{1 + \alpha c_0 K_e} \tag{A4}$$

are given by

$$\lambda_{1,2} = \frac{k_{-1} + k_{-2} + k_1' + k_2'}{2} \pm \frac{1}{2}[(k_{-1} - k_{-2})^2 + (k_{-1} - k_{-2})(k_1' - k_2') + (k_1' + k_2')^2]^{1/2} \tag{A5}$$

When $\alpha \to 1$, the pure (A-T) case, (A5) becomes

$$\lambda_1 = k_{-1} + \frac{k_1 c_0 K_e}{1 + c_0 K_e}$$

$$\lambda_2 = k_{-2} \tag{A6}$$

When $\alpha \to 0$, the pure (G-C) case, (A5) becomes

$$\lambda_1 = k_{-2} + k_2 c_0$$

$$\lambda_2 = k_{-1} \tag{A7}$$

In the derivation of (A5) the free proflavin concentration x has been neglected when summed with y_1 or y_2.

At low phosphate concentration, when k_1' and k_2' are small in relation to k_{-1} and k_{-2}, a suitable approximation for (A5) is

$$\lambda_1 = k_{-1} + \frac{k_1 \alpha c_0 K_e}{1 + \alpha c_0 K_e}$$

$$\lambda_2 = k_{-2} + \frac{k_2(1 - \alpha)c_0}{1 + \alpha c_0 K_e} \tag{A8}$$

In this concentration range the two reactions in (A1) are uncoupled. λ_1 is the reciprocal relaxation time for the binding of dye to pure (A-T) sites of concentration αc_0, and λ_2 is essentially the corresponding parameter for binding to (G-C) sites of concentration $(1 - \alpha)c_0$.

At high phosphate concentration when k_1' and k_2' are large in relation to k_{-1} and k_{-2}, an appropriate approximation for (A5) is instead

$$\frac{1}{\tau_{fast}} = \lambda_1 = k_1' + k_2' + \frac{k_{-1}k_1' + k_{-2}k_2'}{k_1' + k_2'}$$

$$\frac{1}{\tau_{slow}} = \lambda_2 = \frac{k_{-1}k_2' + k_{-2}k_1'}{k_1' + k_2'} \tag{A9}$$

The ratio P_1, where

$$P_1 = \frac{k_1'}{k_1' + k_2'} = \frac{k_1 K_e \alpha}{k_1 K_e \alpha + k_2(1 - \alpha)} \tag{A10}$$

is the probability that the dye from the free state x or the preequilibrium e first goes to an inner (A-T) site. The ratio P_2, where

$$P_2 = \frac{k_2'}{k_1' + k_2'} = \frac{k_2(1 - \alpha)}{k_1 K_e \alpha + k_2(1 - \alpha)} \tag{A11}$$

is the probability that the dye from the free state or the preequilibrium first hits a (G-C) site.

The first eigenvalue in (A9) is the inverse relaxation time for the binding of dye to either (A-T) or (G-C) sites from the free state and the preequilibrium. In the limit $\alpha \to 1$ it corresponds to pure (A-T) binding and in the limit $\alpha \to 0$ to pure (G-C) binding. The second eigenvalue in (A9) is the inverse relaxation time for transfer of proflavin between (A-T) sites and (G-C) sites. The first term is the off rate k_{-1} from an (A-T) site multiplied with the probability of going to a (G-C) site. The second term describes similarly the transfer rate from (G-C) to (A-T) sites. When the (A-T) content is high, $1/\tau_{slow}$ approaches k_{-2}, and when the (G-C) content is high, $1/\tau_{slow}$ approaches k_{-1}:

$$\lim_{\alpha \to 1} 1/\tau_{slow} = k_{-2}$$

$$\lim_{\alpha \to 0} 1/\tau_{slow} = k_{-1} \tag{A12}$$

The total fluorescence intensity at temperature T is given by the concentration of proflavin in its different states and the corresponding fluorescence factors [cf. Rigler & Ehrenberg (1973)]:

$$I = f_x x + f_e e + f_1 z_1 + f_2 z_2 \tag{A13}$$

where

$$f_i = \epsilon_i Q_i \qquad i = x, e, 1, 2 \tag{A14}$$

ϵ_i is the cross section for absorbing a photon from the beam of excitation, and Q_i is the probability of detecting a fluorescence photon from an excited dye molecule.

Define the equilibrium constants K_1 and K_2 from

$$K_1 = k_1/k_{-1} \qquad K_2 = k_2/k_{-2} \tag{A15}$$

The approximations in (A3) lead to simple expressions for all equilibrium concentrations in (A1). In particular

$$z_1 = \frac{x_0 \alpha c_0 K_e K_1}{1 + c_0[\alpha K_e(1 + K_1) + (1 - \alpha)K_2]} = \frac{x_0 \alpha c_0 K_e K_1}{D}$$

$$z_2 = \frac{x_0(1 - \alpha)c_0 K_2}{D} \tag{A16}$$

The total fluorescence intensity is

$$I = \frac{x_0[f_x + f_e \alpha c_0 K_e + f_1 \alpha c_0 K_e K_1 + f_2(1 - \alpha)c_0 K_2]}{D} \tag{A17}$$

The temperature dependence of the equilibrium concentrations is determined by the enthalpic part of the equilibrium constants:

$$K_i(T) = e^{-\Delta H_i/(RT) + \Delta S_i/R}$$

$$\delta K_i = K_i(T + \Delta T) - K_i(T) \qquad i = e, 1, 2 \tag{A18}$$

The concentration shifts for z_1 and z_2 when the temperature is increased from T to $T + \Delta T$ are

$$\delta z_1(0) = z_1(T + \Delta T) - z_1(T)$$

$$\delta z_2(0) = z_2(T + \Delta T) - z_2(T) \tag{A19}$$

The two relations in (A19), which can be explicitly calculated from (A16) and (A18), determine the initial conditions for the differential equations of (A1).

The time variation of the fluorescence after a temperature jump is

$$\Delta I(t) = \delta z_1(t)\left[f_1 - \left(\frac{f_x + f_e\alpha c_0 K_e}{1 + \alpha c_0 K_e}\right)\right] + \delta z_2(t)\left[f_2 - \left(\frac{f_x + f_e\alpha c_0 K_e}{1 + \alpha c_0 K_e}\right)\right] \quad \text{(A20)}$$

If the fluorescence factor f_e of the preequilibrium equals f_x, then (A20) becomes

$$\Delta I(t) = \delta z_1(t)(f_1 - f_x) + \delta z_2(t)(f_2 - f_x) \quad \text{(A21)}$$

We can write

$$\delta z_1(t) = A_1 e^{-\lambda_1 t} + A_2 e^{-\lambda_2 t}$$
$$\delta z_2(t) = q_{21}A_1 e^{-\lambda_1 t} + q_{22}A_2 e^{-\lambda_2 t} \quad \text{(A22)}$$

From matrix diagonalization we obtain

$$A_1 = \frac{q_{22}\delta z_1(0) - \delta z_2(0)}{q_{22} - q_{21}}$$
$$A_2 = \frac{\delta z_2(0) - q_{21}\delta z_1(0)}{q_{22} - q_{21}} \quad \text{(A23)}$$

where

$$q_{22} = \frac{\lambda_2 - a_{11}}{a_{12}} \qquad q_{21} = \frac{\lambda_1 - a_{11}}{a_{12}} \quad \text{(A24)}$$

The coefficients a_{11} and a_{12} are defined by $a_{11} = k_{-1} + k_1'$ and $a_{12} = k_1'$ where k_1' is found in (A4).

The intensity amplitude corresponding to λ_1 is

$$\Delta I_1 = A_1\left[\left(f_1 - \frac{f_x + f_e\alpha c_0 K_e}{1 + \alpha c_0 K_e}\right) + q_{21}\left(f_2 - \frac{f_x + f_e\alpha c_0 K_e}{1 + \alpha c_0 K_e}\right)\right] \quad \text{(A25)}$$

The amplitude corresponding to λ_2 is

$$\Delta I_2 = A_2\left[\left(f_1 - \frac{f_x + f_e\alpha c_0 K_e}{1 + \alpha c_0 K_e}\right) + q_{22}\left(f_2 - \frac{f_x + f_e\alpha c_0 K_e}{1 + \alpha c_0 K_e}\right)\right] \quad \text{(A26)}$$

and the time-dependent fluorescence change is

$$\Delta I(t) = \Delta I_1 e^{-\lambda_1 t} + \Delta I_2 e^{-\lambda_2 t} \quad \text{(A27)}$$

When $\alpha = 1$, the pure (A-T) case, from (A6) and (A23):

$$(\Delta I_1)_{A\text{-}T} = \delta z_1(0)\left[f_1 - \frac{(f_x + c_0 K_e f_e)}{1 + c_0 K_e}\right] \quad \text{(A28)}$$

To simplify, assume that $f_x = f_e$ and that δK_e is negligible in relation to $\delta(K_e K_1)$. Linearization of (A19) renders the approximate relative amplitude

$$\left(\frac{\Delta I_1}{I}\right)_{A\text{-}T} = \frac{c_0(1 + c_0 K_e)(F_1 - 1)\delta(K_e K_1)}{[1 + c_0 K_e(1 + K_1)][1 + c_0 K_e(1 + f_1 K_1)]} \quad \text{(A29)}$$

where $F_1 = f_1/f_x$. When $\alpha = 0$, the pure (G-C) case, from (A7) and (A23)

$$(\Delta I_1)_{G\text{-}C} = \delta z_2(0)(F_2 - 1) \quad \text{(A30)}$$

where $F_2 = f_2/f_x$. The relative amplitude

$$\left(\frac{\Delta I_1}{I}\right)_{G\text{-}C} = \frac{\delta K_2(F_2 - 1)}{(1 + c_0 K_2)(1 + F_2 c_0 K_1)} \quad \text{(A31)}$$

is derived from linearizing (A19).

At high phosphate concentration where k_1' and k_2' dominate over the backrates k_{-1} and k_{-2} from (A9) approximately

$$(\Delta I)_{fast} = [\delta z_1(0) + \delta z_2(0)]\left(P_1 f_1 + P_2 f_2 - \frac{f_x + \alpha c_0 K_e f_e}{1 + \alpha c_0 K_e}\right)$$
$$(\Delta I)_{slow} = [P_2\delta z_1(0) - P_1\delta z_2(0)](f_1 - f_2) \quad \text{(A32)}$$

where P_1 and P_2 are defined by expressions A10 and A11, respectively. In (A32) the backrates k_{-1} and k_{-2} have been neglected when summed with k_1' or k_2'. The amplitude for the fast relaxation time is a combination of (A-T) and (G-C) binding. The higher the (A-T) content the more it resembles (A28), and the higher the (G-C) content the more it goes to (A30). A nonzero amplitude of the slow relaxation time depends on different fluorescence factors f_1 and f_2 for the (A-T) and (G-C) sites, respectively. The term $P_2\delta z_1(0)$ in the first bracket is the transfer from (A-T) sites to (G-C) sites, and the term $P_1\delta z_2(0)$ is a measure of the transfer from (G-C) to (A-T) sites. It is also clear that if the (A-T) sites and the (G-C) sites have identical physical properties and only differ in quantum yields, then $(\Delta I)_{slow}$ is zero since the relation $P_1\delta z_2(0) - P_2\delta z_1(0) = 0$ holds.

References

Albert, A. (1973) *Selective Toxicity*, 2nd ed., Chapman & Hall, London.

Berman, H. M., Carrell, H. L., Glusker, J. P., & Stallings, W. C. (1977) *Nature (London) 269*, 304–307.

Berman, H. M., Stallings, W., Carell, H. L., & Glusker, J. P. (1979) *Biopolymers 18*, 2405–2429.

Blake, A., & Peacocke, A. R. (1968) *Biopolymers 6*, 1225–1253.

Brenner, S., Barnett, L., Crick, F. H. C., & Orgel, A. (1961) *J. Mol. Biol. 3*, 121–124.

Bresloff, J. L., & Crothers, D. M. (1975) *J. Mol. Biol. 95*, 103–123.

Caspersson, T., Zech, L., Wagh, U., Modest, E. J., & Simonsson, E. (1969) *Exp. Cell Res. 58*, 141–152.

Crick, F. H. C., Barnett, L., Brenner, S., & Watts-Tolin, R. J. (1961) *Nature (London) 192*, 1227–1232.

Gale, E. F., Cundliffe, E., Reynolds, P. E., Richmond, M. H., & Waring, M. J. (1972) *The Molecular Basis of Antibiotic Action*, Wiley, New York.

Hogan, M., Dattagupta, N., & Crothers, D. M. (1979) *Biopolymers 18*, 218–288.

Jain, S. C., Tsai, C., & Sobell, H. M. (1977) *J. Mol. Biol. 114*, 317–331.

Lerman, L. S. (1961) *J. Mol. Biol. 3*, 18–30.

Li, H. J., & Crothers, D. (1969) *J. Mol. Biol. 39*, 461–477.

Marquardt, D. W. (1963) *J. Soc. Ind. Appl. Math. 11*, 431–441.

Meeter, D. A. (1964) Non-Linear Least-Squares (Gaushaus), University of Wisconsin Computing Center.

Ornstein, R. L., & Rein, R. (1979) *Biopolymers 18*, 2821–2847.

Pachmann, U., & Rigler, R. (1972) *Exp. Cell Res. 72*, 602–608.

Ramstein, J., & Leng, M. (1972) *Biochim. Biophys. Acta 281*, 18–32.

Ramstein, J., & Leng, M. (1975) *Biophys. Chem. 3*, 234–240.
Ramstein, J., Hélène, C., & Leng, M. (1971) *Eur. J. Biochem. 21*, 125–136.
Ramstein, J., Dourlent, M., & Leng, M. (1972) *Biochem. Biophys. Res. Commun. 47*, 874–882.
Ramstein, J., Houssier, C., & Leng, M. (1973) *Biochim. Biophys. Acta 335*, 54–68.
Rigler, R., & Ehrenberg, M. (1973) *Q. Rev. Biophys. 6*, 139–199.
Rigler, R., Rabl, C. R., & Jovin, T. M. (1974) *Rev. Sci. Instrum. 45*, 580–588.
Seeman, N. C., Day, R. O., & Rich, A. (1974) *Fed. Proc., Fed. Am. Soc. Exp. Biol. 33*, 1537.
Sobell, H. M., Tsai, C., Jain, S. C., & Gilbert, S. G. (1977) *J. Mol. Biol. 114*, 333–365.
Stone, A. L., & Bradley, D. F. (1961) *J. Am. Chem. Soc. 83*, 3627–3634.
Thomes, J. C., Weill, G., & Daune, M. (1969) *Biopolymers 8*, 647–659.
Tsai, C., Jain, S. C., & Sobell, H. M. (1977) *J. Mol. Biol. 114*, 301–315.
Weill, G. (1965) *Biopolymers 3*, 567–572.
Wells, R. D., Larson, J. E., Grant, R. C., Shortle, B. E., & Cantor, C. R. (1970) *J. Mol. Biol. 54*, 465–497.

Mechanism of Benzo[*a*]pyrene Diol Epoxide Induced Deoxyribonucleic Acid Strand Scission†

Howard B. Gamper,* James C. Bartholomew, and Melvin Calvin

ABSTRACT: Approximately 1% of (±)-7β,8α-dihydroxy-9α,10α-epoxy-7,8,9,10-tetrahydrobenzo[*a*]pyrene (BaP-diol epoxide) DNA alkylation sites rearrange with strand scission at neutral pH. Phosphotriester hydrolysis and depurination/depyrimidination strand scission were critically examined as possible mechanisms for this phenomenon. The catalysis of nicking by alkali and the inhibition of nicking by counterions were consistent with either mechanism. The kinetics of nicking, however, were characteristic of a multistep reaction such as depurination/depyrimidination strand scission and the detection of apurinic sites in BaP-diol epoxide alkylated DNA strongly supported this mechanism. The number of such sites, especially at lower reaction levels, was probably sufficient to account for strand scission. No direct evidence was obtained for nicking occurring through phosphotriester hydrolysis. Studies with model substrates, including dibutyl phosphate, DNA homopolymers, and TMV RNA, indicated that if BaP-diol epoxide forms phosphotriesters in DNA or RNA, they do not hydrolyze with strand scission. Besides apurinic/apyrimidinic sites, a second alkali-sensitive rearrangement product was present in BaP-diol epoxide modified DNA. These latter sites accumulated with time and after 24 h accounted for as much as 4% of the initial alkylation events. Although relatively stable at neutrality, they spontaneously nicked the DNA backbone at high pH. It is possible that these sites represent a rearrangement of the major N^2 guanine adduct.

The ubiquitous environmental pollutant benzo[*a*]pyrene is the most widely studied of the carcinogenic polycyclic aromatic hydrocarbons. In mammalian cells it is metabolically activated to either the syn or anti isomers of benzo[*a*]pyrene-7,8-diol 9,10-epoxide (Borgen et al., 1973; Sims et al., 1974; Daudel et al., 1975; King et al., 1976; Ivanovic et al., 1976; Weinstein et al., 1976). Studies have shown this highly reactive electrophile to be cytotoxic (Landolph et al., 1978), mutagenic (Malaveille et al., 1975; Huberman et al., 1976; Wislocki et al., 1976a,b; Wood et al., 1977), transforming in tissue culture (Mager et al., 1977), and tumorigenic in vivo (Levin et al., 1977). It accounts for the majority of DNA and RNA modification (i.e., alkylation or adduct formation) by the hydrocarbon (Koreeda et al., 1978; Vahakangas et al., 1979). The primary adduct in both macromolecules has been shown to consist of a linkage between the C-10 position of the epoxide and the N^2 amino group of guanine (Koreeda et al., 1976; Osborne et al., 1976; Weinstein et al., 1976; Jeffrey et al., 1977; Meehan et al., 1977; Koreeda et al., 1978). The exocyclic amino groups of adenine and probably cytidine are also modified to lesser extents (Jennette et al., 1977; Jeffrey et al., 1977, 1979; Meehan et al., 1977; Straub et al., 1977; Ivanovic et al., 1978).

In a preliminary communication we reported that the synthetic anti isomer (±)-7β,8α-dihydroxy-9α,10α-epoxy-7,8,9,10-tetrahydrobenzo[*a*]pyrene (BaP-diol epoxide)[1] nicked superhelical Col E1 DNA at a low frequency relative to alkylation and proposed a mechanism for nicking based upon the hydrolysis of phosphotriesters rendered unstable by the presence of a β-hydroxyl group on the attached hydrocarbon (Gamper et al., 1977). However, in an independent study Shooter et al. (1977) postulated the same nicking as due to depurination strand scission. Indirect evidence exists for the reaction of BaP-diol epoxide with both DNA phosphate (Koreeda et al., 1976) and the N-7 position of guanine (Osborne et al., 1978; King et al., 1979), a modification known to labilize the glycosidic bond. In this paper we critically assess the relevance of the two proposed mechanisms utilizing as

† From the Laboratory of Chemical Biodynamics, Lawrence Berkeley Laboratory, University of California, Berkeley, California 94720. *Received February 27, 1980.* This research was supported by the Division of Biomedical and Environmental Research, U.S. Department of Energy, under Contract No. W-7405-ENG-48.

[1] Abbreviations used: BaP-diol epoxide, (±)-7β,8α-dihydroxy-9α,10α-epoxy-7,8,9,10-tetrahydrobenzo[*a*]pyrene; BaP-tetraol, 7,8,9,10-tetrahydroxy-7,8,9,10-tetrahydrobenzo[*a*]pyrene; Hepes, *N*-2-hydroxyethylpiperazine-*N'*-ethanesulfonic acid.

0006-2960/80/0419-3948$01.00/0